Tunnelling and Underground Space Technology 95 (2020) 103128

Contents lists available at ScienceDirect

Tunnelling and Underground Space Technology

journal homepage: www.elsevier.com/locate/tust

Experimental and performance analysis of reverse circulation reaming in horizontal directional drilling

Shun Dong[a], Cong Zeng[a,*], Samuel T. Ariaratnam[b], Baosong Ma[a], Xuefeng Yan[a], Zhijie Li[a], Xinjie Li[a]

[a] College of Engineering, China University of Geosciences-Wuhan, No. 388 Lumo Road, Wuhan, Hubei Province, China
[b] School of Sustainable Engineering and the Built Environment, Arizona State University, 660 S. College Ave., Tempe, AZ, United States

ARTICLE INFO

Keywords:
Horizontal directional drilling
Reverse circulation
Jet-pump design theory
Lab scale reamer

ABSTRACT

To overcome the inefficient cuttings transportation performance of current large-diameter Horizontal Directional Drilling (HDD), the application of reverse circulation technology during the reaming process was studied resulting in the development of a novel reverse-circulation reamer. A prototype lab-scale reamer was developed in accordance with jet-pump design theory and project requirements. An experimental laboratory setup was developed to simulate the reverse circulation reaming process, through which parametric studies were performed to investigate the effects of various operating conditions on the reamer's performance and cuttings removal ability. The experimental results concluded that the reamer's non-cavitating performance kept constant with variations in operating conditions, while its anti-cavitation ability was reduced by increasing the primary flow rate or decreasing the suction pressure. Comparisons of non-cavitating experimental data with various theoretical correlations were conducted and Cunningham's model was founded to be most applicable. In addition, a critical rotatory speed was identified at which the reamer's ability to transport cuttings is most effective.

1. Introduction

Horizontal Directional Drilling (HDD) is a trenchless construction method typically used for the installation of pipelines and conduits, with particular benefits for crossing under rivers, lakes or other areas where open-cut construction may be challenging (Faghih et al., 2015; Rostami et al., 2015). A demand for greater petroleum, natural gas, and water transportation capacity has resulted in an increase in large-diameter HDD crossing projects in Mainland China (Carlin and Ariaratnam, 2018; Ma and Najafi, 2008). Before the pipeline installation, a pilot hole is drilled and then reamed, typically up to a diameter 50% larger than the size of the product pipe (Rabiei et al., 2018). During current reaming practices, drilling fluid with cuttings (i.e. slurry) returns to the surface through the annulus between the drill pipe and borehole with its velocity dropping dramatically with increase in borehole diameter (Rostami et al., 2017; Shu et al., 2014). Under a low flow velocity, solid phase within the drilling fluid tends to settle and accumulate at the bottom of the borehole, thereby creating a cuttings bed (Ariaratnam et al., 2007). The formation of a cutting bed often creates problems including decrease in the reaming efficiency and damage on the product pipe or drill pipe fracture resulting in increased project duration and cost.

Reverse circulation drilling refers to a drilling approach which involves circulating the clean drilling fluid through the annulus to the bottom of the borehole and bringing the cuttings back to the surface through the drill pipe (Zhu et al., 2015). Due to its advantages over conventional drilling, reverse circulation drilling has been used in numerous areas including geological investigation and oil exploration, resulting in significant economic benefits. Strauss et al. (1989) reviewed several case studies where dual-wall air reverse circulation was applied in ground water exploration in Southern California. Morrison et al. (1987) set up an experimental apparatus to study the impacts of jet port number and air flow rate on the efficiency of air lift reverse circulation. Livingstone (2007) proposed a reverse circulation method for drilling a directional or horizontal wellbore in a hydrocarbon formation using concentric drill pipe to reduce the accumulation of drill cuttings. Bo et al. (2011) used reverse circulation DTH hammer drilling for geological core exploration in complex strata and the average drilling efficiency was increased by 64%. Gan et al. (2015) innovatively designed a large-diameter reverse circulation drill bit for oil and gas exploration with an average penetration rate of 4.5 m/h being reached in the field drilling tests.

* Corresponding author.
E-mail addresses: zengcong@126.com (C. Zeng), ariaratnam@asu.edu (S.T. Ariaratnam).

https://doi.org/10.1016/j.tust.2019.103128
Received 4 April 2019; Received in revised form 15 August 2019; Accepted 16 September 2019
Available online 25 October 2019
0886-7798/

Several researchers have also made attempts to use reverse circulation technology for wellbores cleaning. Kumar et al. (2005) carried out coiled tubing reverse circulation trials to establish an effective method for cleaning petroleum horizontal wells and an average increase of 15% in water injection rate was indicated. Li et al. (2010) established an experimental setup to simulate the cleaning process of horizontal wellbores with coiled tubing reverse circulation and developed empirical correlations to enable the optimization of the process. Liu and Xia (2009) used pump suction reverse circulation to clean the horizontal borehole in rock strata and obtained a satisfying cuttings removal efficiency. Herrenknecht developed a downhole jet pump (DHJP) for full face pilot hole boring or borehole cleaning, with which a clean borehole was created (Madryas et al., 2017).

The successful applications in these areas provide the motivation to propose reverse circulation reaming to improve the cuttings transportation efficiency of large-diameter HDD reaming. In addition to facilitating cuttings removal, the proposed reverse circulation reaming can also reduce the risk of formation fracturing due to over-pressurizing the borehole since the annular pressure is equal to the surrounding ground level water; and reduce the drilling fluid program, thereby resulting in reduced mud disposal. To achieve the proposed process, a new reverse circulation reamer was designed based on jet-pump design theory. Laboratory experiments were then conducted to study the reamer's performance and cuttings removal ability.

2. HDD reverse circulation reaming

2.1. Jet-pump design theory

A jet pump, schematic represented in Fig. 1, typically consists of nozzle, suction chamber, throat and diffuser (Lima Neto and Melo Porto, 2004). Pump behavior is generated after the high-pressure primary flow issuing from the nozzle in the form of a high-velocity jet, resulting in the secondary flow pumped into the suction chamber and mixed with the primary flow. Energy and momentum transfer between the primary and secondary flow occurs within the throat to form a homogenous mixture, of which the static pressure is raised by the divergent diffuser (Cunningham and River, 1957; Reddy and Kar, 1968).

There are number of fundamental jet pump parameters, all expressed in dimensionless form. These parameters are defined as follows in Eqs. (1)–(4):

$$\text{Area ratio:} \quad m = \frac{A_t}{A_n} \tag{1}$$

$$\text{Flow ratio:} \quad q = \frac{Q_s}{Q_n} \tag{2}$$

$$\text{Head ratio:} \quad h = \frac{H_o - H_s}{H_n - H_s} \tag{3}$$

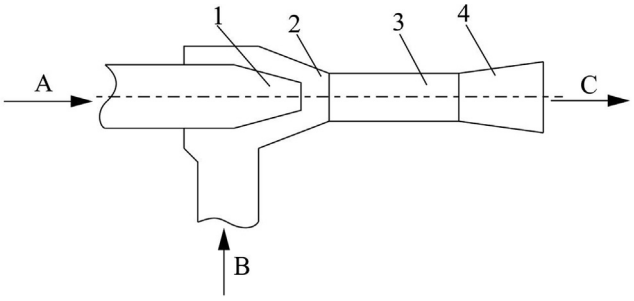

1-Nozzle, 2-Suction chanber, 3-Throat, 4-Diffuser
A-Primary flow, B-Secondary flow, C-Delievery flow

Fig. 1. Schematic representation of jet pump.

$$\text{Efficiency:} \quad \eta = q\frac{h}{1-h} \tag{4}$$

where Q is the volumetric flow rate, H is the hydraulic head, A is the cross-section area. Subscript t refers to the throat, n refers to the nozzle, s refers to the suction inlet and o refers to the jet pump's outlet. The performance of jet pump is generally represented by a q-h correlation, which was first introduced by Gosline and O'Brien (1934). Using theoretical analysis and a series of experiments, Lu and Zeng (1981) derived a q-h correlation with the consideration of nozzle-to-throat distance and simplified it to:

$$h = \varphi_1^2 \frac{h_0}{q_0}(q_0 - q) \tag{5}$$

$$q_0 = (5m - 0.9445)^{0.5} - 1.75, \ (m = 1.5\ 3.0) \tag{6}$$

$$h_0 = 2.667 - 0.00253(m + 26.07)^2, \ (m = 1.5\ 3.0) \tag{7}$$

$$q_0 = (5m - 0.9445)^{0.5} - 1.7, \ (m = 3.0\ 25) \tag{8}$$

$$h_0 = 1.45m^{-0.892}, \ (m = 3.0\ 25) \tag{9}$$

where φ_1 is the friction loss coefficient at the nozzle. Based on Eqs. (5)–(9), Lu and Zeng (1981) suggested the following Eq. (10) to determine the jet pump's optimal area ratio, m_y.

$$m_y = \frac{0.95\varphi_1^2}{h + 0.003\varphi_1^2} \tag{10}$$

2.2. Reverse circulation reamer prototype

In HDD reaming operations, the front and rear of the reamer is usually connected with drill pipe, thereby offering a complete flow channel for drilling fluid transportation. Given this characteristic, a reverse circulation reamer was devised as illustrated in Fig. 2. The proposed reamer is a combination of a conventional HDD reamer and jet pump, and is composed of roller bits, suction inlets, nozzle, suction chamber, throat and diffuser.

With a conventional reaming method, drilling fluid pumped by the drill rig enters the borehole through a set of nozzles distributed on the reamer, and flows through the annulus between the drill pipe and borehole to the surface with cuttings being carried as demonstrated in Fig. 3a. With the proposed reverse circulation reamer, drilling fluid pumped by the drill rig works as primary flow and ejects at the nozzle to generate a low-pressure zone within the suction chamber. Due to the pressure difference between the borehole and suction chamber, drilling fluid in the annulus is pumped into the reamer and cuttings are entrained. The slurry mixture returns to the ground through the drill pipe connected behind the reamer as illustrated in Fig. 3b. The drill pipe's small diameter enables the drilling fluid within the drill pipe to gain a high velocity and flows in a turbulent state, which is conducive to cuttings transportation.

The proposed reaming process also differs from the reverse circulation drilling or borehole cleaning. Firstly, dual-wall drill pipe is used in reverse circulation drilling. The fluid is pumped through its annulus and drill cuttings are returned to the surface through its inner pipe. But for the proposed reverse circulation reaming, dual-wall drill pipe is not needed since the fluid is pumped through drill pipe connected with the front of the reamer and the cuttings are entrained to the surface through drill pipe connected with the rear of the reamer. Secondly, the pump behavior in reverse circulation borehole cleaning is created by the pump on the ground, while it is generated by the high-pressure drilling fluid ejecting in the reverse circulation reaming. Thirdly, the downhole jet pump developed by Herrenknecht is either used to achieve full face pilot hole boring or used as a borehole cleaning tool, while the proposed reverse circulation reamer is used in the reaming process.

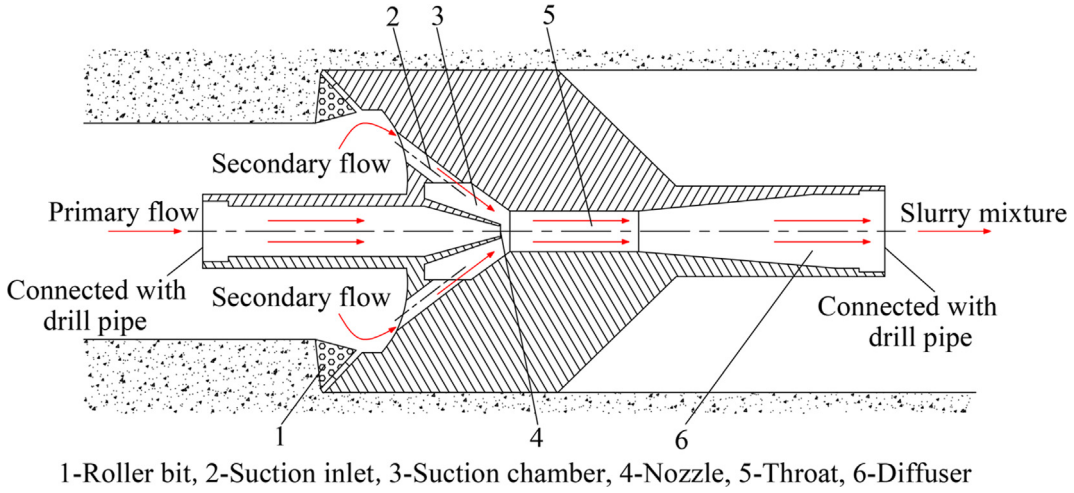

Fig. 2. Sketch of the proposed HDD reverse circulation reamer.

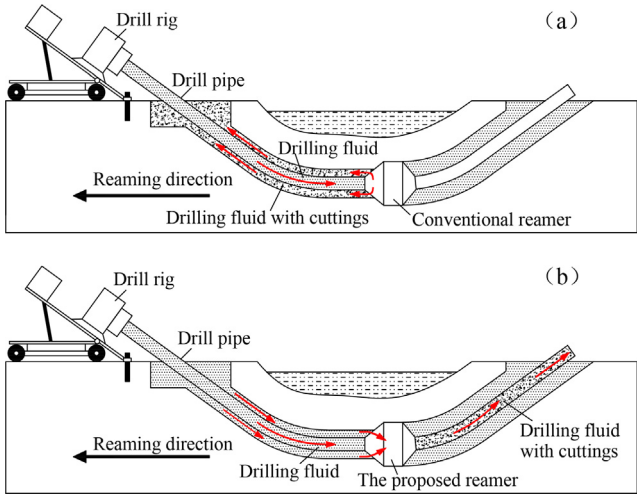

Fig. 3. Comparison of drilling fluid flow direction.

2.3. Geometric parameters

A 2000 m long HDD installation of natural gas pipeline is planned for late 2019 in a suburban area of Beijing, China. The product pipe diameter is 1016 mm and the selected drill pipe's inner diameter is 150 mm. Geotechnical investigations reveal that the crossing strata is sedimentary rock with a number of fracture zones and dominated by volcanic tuff. Elevation difference between the entry and exit point is approximately 23 m. Before installation of the product pipe, the drilled pilot hole is pre-reamed using a sequence of 508 mm, 762 mm, 914 mm, 1067 mm, 1168 mm, 1270 mm and 1372 mm diameter reamers. The reaming passes with diameter below 800 mm are back reamed with a mud motor, while the proposed reverse circulation reaming will be used for the other passes. Project parameters used in the reamer's geometry determination are summarized in Table 1.

To ensure that the cuttings can be effectively transported to the surface, the slurry mixture's critical velocity and overall head loss within the drill pipe must be calculated. Critical velocity, U_C, is defined as the minimum velocity differentiating flows in which the solids form a bed at the bottom of the pipe from fully suspended flows and can be estimated by the empirical correlation put forward by Turian et al. (1987).

$$\frac{U_C}{[2gD(s-1)]^{0.5}} = 8.948C^{0.4779}C_D^{-0.0272}\left\{\frac{D\rho[gD(s-1)]^{0.5}}{\mu}\right\}^{-0.1174} \tag{11}$$

Table 1
Parameters used in the reamer's geometry determination.

Parameters	Symbol	Units	Value
Length of borehole path	L	m	2000
Burial depth of borehole path	H_D	m	7.5
Drill pipe's inner diameter	D	mm	150
Viscosity of drilling fluid (water)	μ	mPa·s	0.8949
Unit weight of drilling fluid (water)	γ	kN/m^3	9.97
Fluid pressure by drill rig	H_R	m	300

where D is the drill pipe's diameter, C is the solid concentration, μ is the drilling fluid's viscosity, s is the solid to liquid density ratio , C_D is the drag coefficient for free-falling particle and ρ is the drilling fluid's density.

The slurry's overall head loss, H_M, is composed of major loss, H_F, and minor loss, H_L.

$$H_M = H_F + H_L \tag{12}$$

H_F is the head loss due to viscous effects in the straight drill pipes and can be determined by:

$$H_F = i_F L \tag{13}$$

where L is the length of borehole path, i_F is the gradient of frictional head loss and can be measured by Zandi and Govato's (1967) approach which is given as follows:

$$\frac{i - i_w}{i_w C} = 280\varphi^{-1.93} \quad for \quad \varphi < 10 \tag{14}$$

$$\frac{i - i_w}{i_w C} = 6.30\varphi^{-0.354} \quad for \quad \varphi > 10 \tag{15}$$

in which φ is expressed by:

$$\varphi = \frac{U^2}{gD(s-1)}C_D^{\frac{1}{2}} \tag{16}$$

where U is slurry's mean velocity within drill pipe.

H_L is the head loss caused by the joints and bends of drill pipes and can be determined by Munson et al. (2006).

$$H_L = \xi_1\frac{U^2}{2g}\frac{\gamma_m}{\gamma}\cdot n + \xi_2\frac{U^2}{2g}\frac{\gamma_m}{\gamma} \tag{17}$$

in which γ_m and γ is the unit weight of the slurry and drilling fluid, n is the number of joints, ξ_1 and ξ_2 are the loss coefficients.

With the parameters presented in Table 1 and Eqs. (11)–(17), the slurry's overall head loss and critical velocity are estimated. Then the

required hydraulic head, H_o, and volumetric flow rate, Q_o, at the reamer's outlet can be computed by:

$$H_o = H_M \tag{18}$$

$$Q_o = \frac{\pi D^2}{4} U_C \tag{19}$$

The hydraulic head at the nozzle, H_n, can be approximated by the fluid pressure provided by drill rig, H_R. The hydraulic head at the suction inlet, H_s, is equal to the burial depth of the borehole path, H_D. With H_n, H_s, H_o and Q_o, the reamer's geometric parameters can be calculated with the following steps:

1) calculate the reamer's head ratio with Eq. (3).
2) calculate the corresponding optimal area ratio with Eq. (10).
3) calculate the corresponding flow ratio with Eqs. (5)–(9).
4) calculate the primary flow rate with Eqs. (2) and (20).

$$Q_o = Q_n + Q_s \tag{20}$$

5) calculate the nozzle diameters, d_1, by:

$$d_1 = \sqrt{\frac{4Q_n}{\pi\varphi_1\sqrt{2gH_n}}} \tag{21}$$

6) calculate the throat diameters, d_2, by:

$$d_2 = d_1\sqrt{m_y} \tag{22}$$

7) the nozzle-to-throat spacing, L_1, throat's length, L_2, nozzle angle, θ_1, and diffuser angle, θ_2, recommended by Lu and Zeng (1981) range from 1–2d_1, 5–7d_2, 20–40° and 8–10° respectively, with the medians of the ranges used in this research. The obtained geometric parameters are presented in Table 2.

3. Experimental system and equipment

3.1. Experimental setup

To investigate the reamer's performance, a laboratory experimental system (schematically shown in Fig. 4) was established. Working fluid in the water tank 1 is pumped into the lab scale reamer 14 by a high-lift centrifugal pump 2 with its volumetric flow rate controlled by a bypass valve 3 and a frequency controller. Because of the pump behavior generated by the high-speed ejecting of the primary fluid at the nozzle, fluid within the pipe 13 is sucked into the lab scale reamer 14 resulting in a pressure reduction in the pipe 13. To keep a constant suction pressure for the lab scale reamer 14, a low-lift centrifugal pump 21 is used to provide secondary flow, where its volumetric flow rate is controlled by a bypass valve 20 and a frequency controller. The discharge flow returns to the water tank 1 to form a loop and its pressure is regulated by a control valve 19. The flow rate and static pressure at the lab scale reamer's inlet is measured by a pressure gauge 6 and an electromagnetic flowmeter 4, while the flow rate and static pressure at the outlet is measured by a pressure gauge 17 and an electromagnetic flowmeter 18. Suction pressure is measured by a pressure gauge 12 at the pipe's crown. To simulate the reamer's rotation, an electromotor 5 is used to actuate the lab scale reamer 14, and its rotary speed, measured by a hall sensor 10, is controlled by a gear box 8 and a frequency controller.

Table 2
Geometric parameters of the reverse circulation reamer.

Parameters	Symbol	Units	Value
Nozzle diameter	d_1	mm	18
Throat diameter	d_2	mm	33
Nozzle-to-throat spacing	L_1	mm	27
Throat length	L_2	mm	198
Diffuser length	L_3	mm	267
Nozzle length	L_4	mm	106
Diffuser angle	θ_1	degrees	9
Nozzle angle	θ_2	degrees	30

Cuttings transportation efficiency, η_p, is considered as a critical indicator of the reamer's feasibility and is quantified by the ratio of transported particles mass to injected particles mass. To examine the reamer's η_p, previous experimental setup was retrofitted. In the retrofitted setup, Silica particles are injected through the valve mounted at the pipe's crown (Fig. 5). A funnel for particle injecting and two devices for cuttings collection are added. Some of the injected silica particles are pumped into the reamer, transferred out of the pipe and then collected by a cuttings collection device, while others left within the pipe are flushed out through the valve mounted at the pipe's bottom and blocked by the other cuttings collection device. Given the challenges of simulating the HDD reaming operation in laboratory, two modifications are made in the experiment. One is that the silica particles are injected through the valve at the pipe's crown instead of along the pipe's circumference. The other is that a small gap between the lab scale reamer and pipe exists for reducing the rotation resistance.

3.2. Lab scale reamer

Given the limited pumping capacity of the existing centrifugal pumps, a lab scale reamer (Fig. 6) with scaled dimensions is 3-D printed with a precision of ± 0.15 mm and dimensions are listed in Table 3. The experiment only considers the cuttings transportation process resulting in the roller bits being replaced for simplification.

3.3. Test equipment

Two DN-15 LDG electromagnetic flowmeters are used in the experiment and installed horizontally with 150 mm straight pipe in the front and 75 mm straight pipe in the rear. The flowmeter's upper and lower limits are 15 m/s and 0.3 m/s respectively, and its measurement error is significantly decreased by the increase in flow velocity as illustrated in Fig. 7. Before the experiment, an ultrasonic flowmeter with standard S1 sensors is installed on the driving and delivery line to verify the electromagnetic flowmeters' accuracy (Fig. 8). The ultrasonic flowmeter's upper and lower limits are 32 m/s and 0.01 m/s respectively, with a precision of 1%. Three MD-S260 digital pressure gauges, with a precision of 1%, are used in the experiment for fluid pressure monitoring. The one with a measurement range from 0 to 1.6 MPa is mounted near the lab scale reamer's inlet, while the other two gauges with a measurement range from 0 to 0.4 MPa are mounted at the pipe's crown and the reamer's outlet respectively.

3.4. Experimental procedure

The experimental procedure applied to investigate the prototype reverse circulation reamer's performance is detailed as follows:

1) fully open the reamer's discharge valve and turn on the pumps;
2) adjust the primary flow rate and suction pressure;
3) close the reamer's discharge valve gradually;
4) record the readings of flowmeters and pressure gauges when a steady state is obtained;
5) steps 1 to 4 are repeated under different operating conditions.

The experimental procedure to investigate the prototype reverse circulation reamer's cuttings transportation ability is detailed as follows:

1) fully open the reamer's discharge valve and turn on the pumps;
2) adjust the primary flow rate and suction pressure;

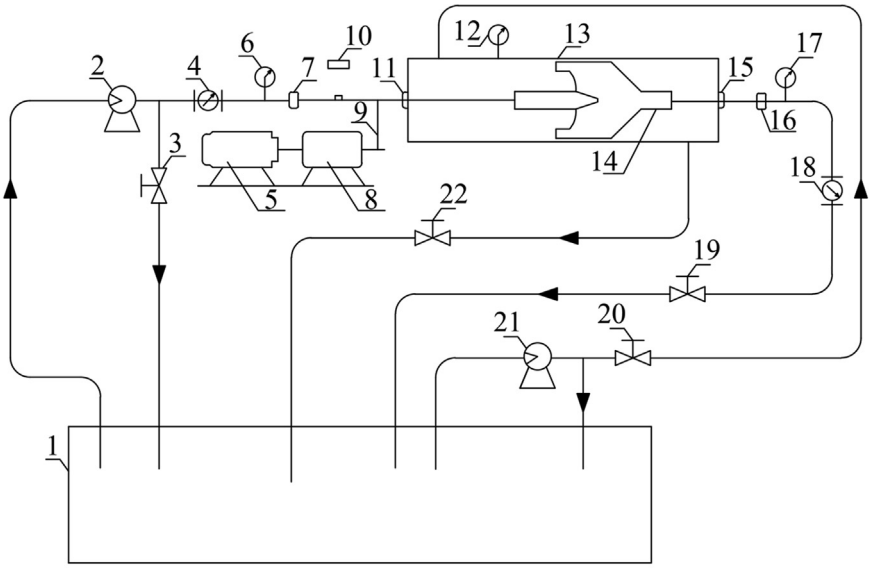

1-Water tank，2、21-Centrifugal pump，3、19、20、22-Valve，4、18-Electromagnetic flowmeter，5-Electromotor、6、12、17-Pressure gauge，7、16-Rotation separator，8-Gear box，9-Chain，10-Hall sensor，11、15-Mechanical seal，13-Pipe、14-Lab Scale reamer

Fig. 4. Schematic diagram of the experimental system.

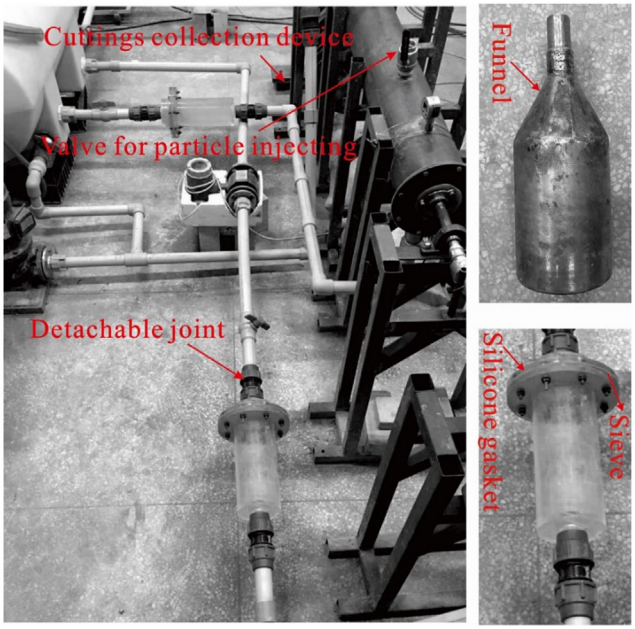

Fig. 5. The retrofitted experimental setup for cuttings transportation experiment.

3) add the weighted particles into the pipe through the funnel;
4) close the discharge valve and open the drain valve;
5) collect the transported particles;
6) steps 1 to 5 are repeated under different operating conditions.

4. Experimental results and discussions

In this research, the proposed reverse circulation reamer is studied experimentally to investigate its performance and cuttings transportation ability. The results are shown in the following sections.

4.1. Non-cavitating and cavitating performance

Similar to jet pump, non-dimensional curves q-h and q-η are used to evaluate the reamer's performance and regression analysis of the non-cavitating experimental data is also performed.

4.1.1. Primary flow rate

To investigate the impacts of the primary flow rate, Q_n, on the reamer's performance, four different Q_n of 2.29 m^3/h, 3.05 m^3/h, 3.56 m^3/h and 3.82 m^3/h are selected while the suction pressure is kept constant as atmospheric pressure. Fig. 9a presents the experimental q-h results under different Q_n, and the corresponding q-η results are shown in Fig. 9b. Fig. 9a also represents a best q-h fit curve for the non-cavitating experimental data and Fig. 9b represents the corresponding efficiency curve.

As illustrated in Fig. 9, the experimental data obtained under different Q_n shares the same trend. Specifically, the flow ratio, q, increases linearly with the decrease of head ratio, h, under non-cavitating conditions, and then q reaches a peak value (the limit ratio q_k) and keeps constant while h keeps on decreasing under cavitating conditions. Regression analysis of the non-cavitating experimental data illustrates a preferable linear relationship between q and h. The results are presented in Table 4. It is clear that the primary flow rate does not obviously impact the reamer's non-cavitating performance because the linear regression results are close (i.e. the maximum discrepancy for intercept is 0.46% and the maximum discrepancy for slope is 5.5%) as Q_n varies from 2.29 m^3/h to 3.82 m^3/h. By contrast, a distinct effect of Q_n on the reamer's cavitating performance is observed in Fig. 9. On the one hand, the reamer's limit flow ratio, q_k, is reduced by the increase of Q_n. For example, for Q_n = 2.29 m^3/h the q_k is 1.27; reduces to 1.06 with a drop of 16.5% for Q_n = 3.05 m^3/h, and decreases by 16.03% to 0.89 for Q_n = 3.56 m^3/h. On the other hand, the critical head ratio, h_c, (defined as the point below which cavitation occurs) decreases with the drop of Q_n. As Q_n decreases from 3.82 m^3/h to 3.05 m^3/h, h_c drops to 0.16 from 0.22; when Q_n reduces to 2.29 m^3/h, no cavitation is observed. The increase of Q_n facilitates the occurrence of cavitation and undermines the reamer's anti-cavitation capability. This can be explained by the fact that a higher Q_n produces lower levels of static pressure in the reamer's suction chamber (due to a higher jet velocity)

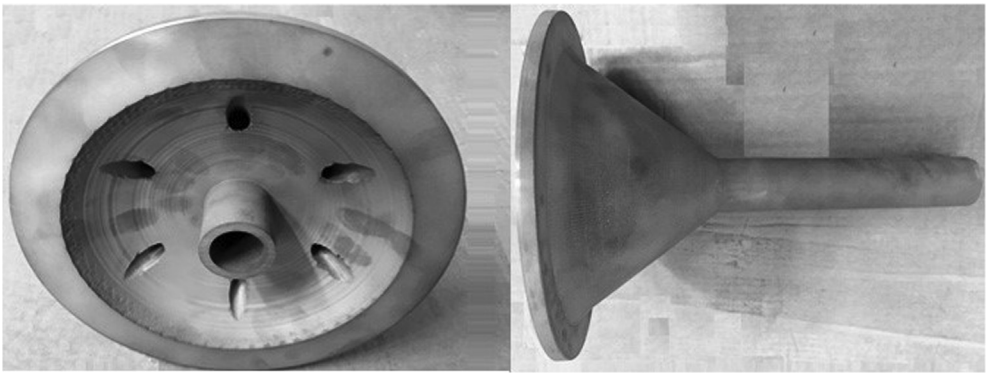

Fig. 6. The lab scale reamer manufactured by 3-D printing (200 mm diameter/500 mm length).

Table 3
Dimensions of the real vs. lab scale reamers.

Reamer	d_1(mm)	d_2(mm)	L_1(mm)	L_2(mm)	L_3(mm)	L_4 (mm)
Real reamer	18	33	27	198	267	106
Lab scale reamer	6	11	9	66	89	35.3

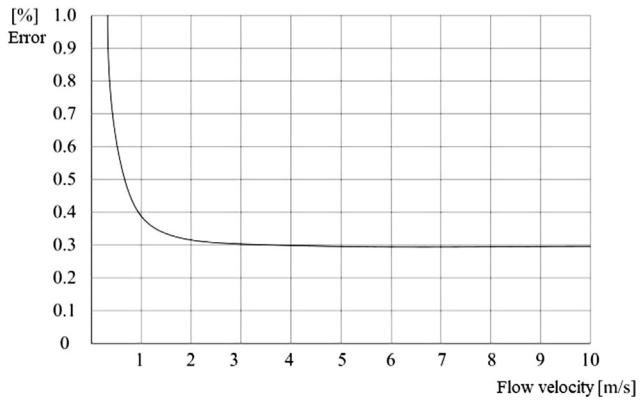

Fig. 7. Variation of the measurement error over flow velocity.

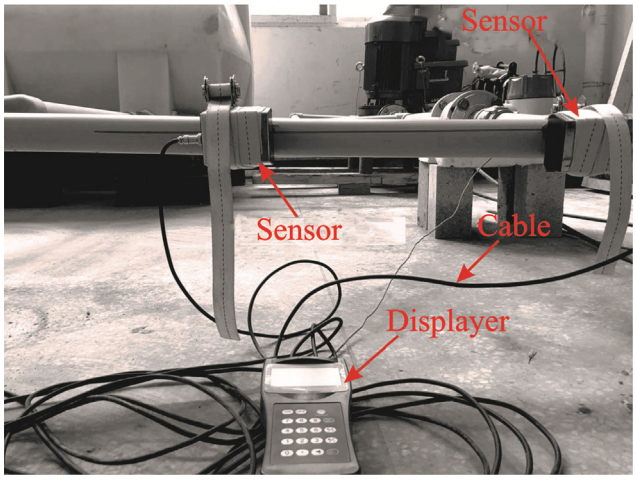

Fig. 8. Ultrasonic flowmeter installed on the driving line.

and a lower axial pressure gradient in the throat. Both effects are conducive to cavitation.

4.1.2. Suction pressure

To investigate the impacts of the suction pressure, P_s, on the reamer's performance, three different P_s of 25 kPa, 75 kPa and 125 kPa are chosen while Q_n is maintained at 3.56 m^3/h. The variations of the reamer's performance over P_s are shown in Fig. 10. Indistinctive discrepancy in non-cavitating performance between different P_s is illustrated in Fig. 10, and confirmed by the regression results presented in Table 5. All the non-cavitating experimental data is linearly fitted and the resulting intercept as well as slope is 0.436, −0.263 respectively shown in Fig. 10a. Also illustrated in Fig. 10 is a distinct effect of P_s on the reamer's cavitating performance. Namely, a higher P_s produces a higher q_k and a lower h_c. Specifically, as P_s increases from 25 kPa to 75 kPa, q_k grows from 1.03 to 1.26 and h_c drops from 0.15 to 0.11 respectively. As P_s reaches 125 kPa, no obvious cavitation is observed. In general, increasing P_s reinforces the reamer's anti-cavitation capability, which is opposite to the role played by Q_n. During the reverse circulation reaming process, the reamer's anti-cavitation performance improves with an increase in borehole depth.

4.1.3. Reamer's rotation

During the HDD reaming process, the rotation of the reamer is driven by drill rig to enlarge the borehole. To study the impacts of the reamer's rotation on its performance, the reamer in the experiment is actuated to rotate by a motor and the rotary speed, n, is set to vary from 20 r/min to 80 r/min with an interval of 20 r/min while Q_n and P_s are kept constant at 3.56 m^3/h and atmospheric pressure, respectively. As demonstrated in Fig. 11, all experimental points obtained under non-cavitating and cavitating conditions almost overlap, suggesting that the reamer's rotation has no impact on its non-cavitating or cavitating performance. Regression analysis for the non-cavitating experimental points measured under various n was performed, and no distinction is indicated as presented in Table 6.

4.1.4. Comparison with theoretical correlations

The non-cavitating experimental data is compared with the theoretical q-h correlations developed by Gosline and O'Brien (1934), Cunningham and River (1957), Lu and Zeng (1981), and the results are demonstrated in Fig. 12. Two observations can be made from Fig. 12a. The first is that q-h curves from the theoretical correlations are close to straight lines, and that Gosline and Cunningham's correlations are almost parallel. Second, Cunningham's correlation generally agrees better with the experimental data than the other two correlations. One possible reason is that the nozzle-to-throat space is considered in Cunningham's correlation while the nozzle is assumed to be in the fully inserted position in Gosline's correlation. Moreover, the reamer's efficiency is well predicted by the theoretical correlations as q is less than 0.45. However, once q exceeds 0.45 Gosline and Lu and Zeng's correlations diverge from the experimental data, these divergences are intensified by increase in q as shown in Fig. 12b.

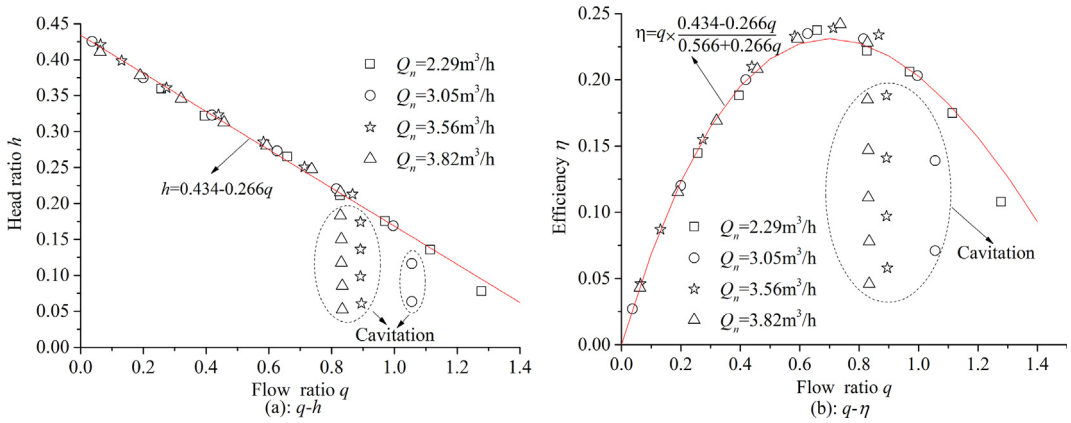

Fig. 9. Performance curves (a: *q-h*, b: *q-η*) of the reamer under various primary flow rates.

Table 4
Regression results of non-cavitating experimental data under different Q_n.

Primary flow rate (Q_n)	Intercept		Slope		Adj. R-Square
	Value	Standard error	Value	Standard error	
2.29 m^3/h	0.434	0.00685	−0.271	0.00799	0.99481
3.05 m^3/h	0.433	0.00293	−0.262	0.00477	0.99834
3.56 m^3/h	0.434	0.00170	−0.256	0.00328	0.99901
3.82 m^3/h	0.432	0.00105	−0.268	0.00231	0.99954
Average	*0.434*	*0.00222*	*−0.266*	*0.00348*	*0.99574*

Table 5
Regression results of non-cavitating experimental data under different P_s.

Suction pressure (P_s)	Intercept		Slope		Adj. R-Square
	Value	Standard error	Value	Standard error	
25 kPa	0.433	0.00146	−0.252	0.00249	0.99941
75 kPa	0.435	0.00238	−0.259	0.00320	0.99878
125 kPa	0.432	0.00324	−0.260	0.00412	0.99750
Average	*0.436*	*0.00180*	*−0.263*	*0.00252*	*0.99698*

4.2. Cuttings transportation efficiency

4.2.1. Particle size

Three particle sizes of 0.5–1 mm, 1–2 mm and 2–4 mm are used in the experiment, with the experimental results illustrated in Fig. 13. As demonstrated in Fig. 13, an increase in particle size results in a general drop in the cuttings transportation efficiency, η_p. As the particle size increases from 0.5–1 mm to 2–4 mm, the average and maximum η_p drops 18.7% and 19.5% respectively. This is expected because particles with a larger size settle faster and are less likely to be pumped into the reamer. Meanwhile, a similar trend that η_p increases to reach a peak value and then drops over the increase in rotary speed is also indicated, but the critical rotary speed, n_c, at which the maximum η_p is achieved shifts from 20 r/min for 0.5–1 mm particle to 40 r/min for 2–4 mm particle. One possible explanation could be that the injected particles tend to settle at the bottom of the pipe due to gravitation, while they are also forced by the fluidic drag to move with the fluid (against the settlement). At critical rotary speed, these two movements are properly balanced and the highest η_p is achieved. For larger particles, a greater n_c will be required to balance the gravitational settlement since the increase in particle size causes an increase in settling velocity.

4.2.2. Drilling fluid

To investigate drilling fluid's impacts on the reamer's cuttings transportation efficiency, η_p, two types of bentonite drilling fluid were also used in the experiment. Table 7 presents the drilling fluid ingredients and properties that were measured by a Marsh Funnel and 6-speed rotary viscometer.

Fig. 14 shows the variations of η_p with different drilling fluids. This further confirms the importance of drilling fluid in promoting cuttings transportation. The shift from water to #1 drilling fluid leads an increase of 14.8% in the average η_p from 36.8% to 51.6%. A further increase in the average η_p from 51.6% with #1 drilling fluid to 65.2% with #2 drilling fluid is also observed. This can be explained by the fact that drilling fluid with a greater viscosity is more capable of suspending particles resulting in cuttings more likely to be pumped into the reamer. Another observation is that the maximum η_p is achieved at non-rotation

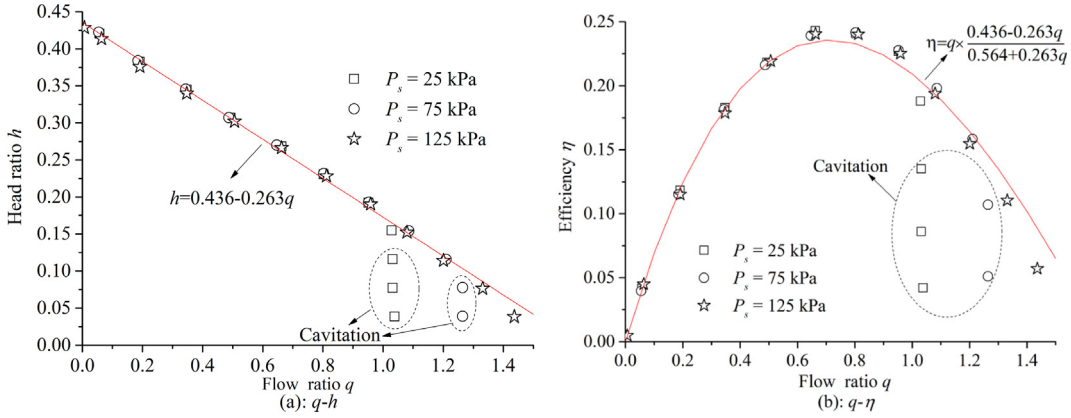

Fig. 10. Performance curves (a: *q-h*, b: *q-η*) of the reamer under various suction pressures.

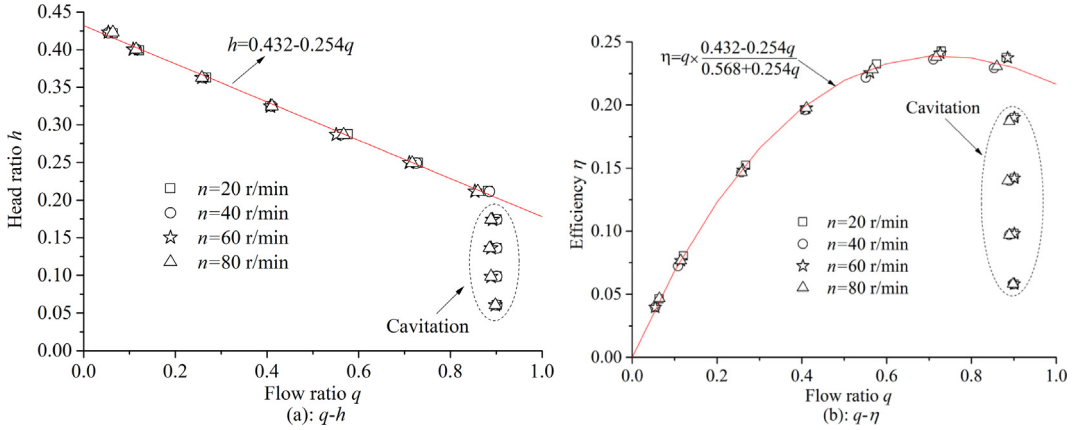

Fig. 11. Performance curves (a: q-h, b: q-η) of the reamer under various rotary speeds.

Table 6
Regression results of non-cavitating experimental under different rotary speeds.

Rotary Speed (n)	Intercept		Slope		Adj. R-Square
	Value	Standard error	Value	Standard error	
20 r/min	0.432	0.00259	−0.261	0.00496	0.99765
40 r/min	0.431	0.00241	−0.260	0.00465	0.99794
60 r/min	0.431	0.00227	−0.258	0.00449	0.99819
80 r/min	0.433	0.00262	−0.258	0.00512	0.99764
Average	*0.432*	*0.00124*	*−0.259*	*0.00241*	*0.99758*

condition as bentonite drilling fluid is used.

5. Conclusions and recommendations

In this paper, experiments were conducted to investigate the performance and cuttings transportation ability of a proposed reverse circulation reamer, and to compare the non-cavitating experimental data with different theoretical correlations. The following conclusions are made based on the research:

1. Neither the primary flow rate, Q_n, nor the suction pressure, P_s, makes a difference in the reamer's non-cavitating performance; however, the growth in Q_n or reduction in P_s decreases the limit ratio and increases the corresponding critical head ratio, thereby undermining the reamer's anti-cavitation capability. Furthermore, the reamer's rotation does exert influence on its non-cavitating or cavitating performance.

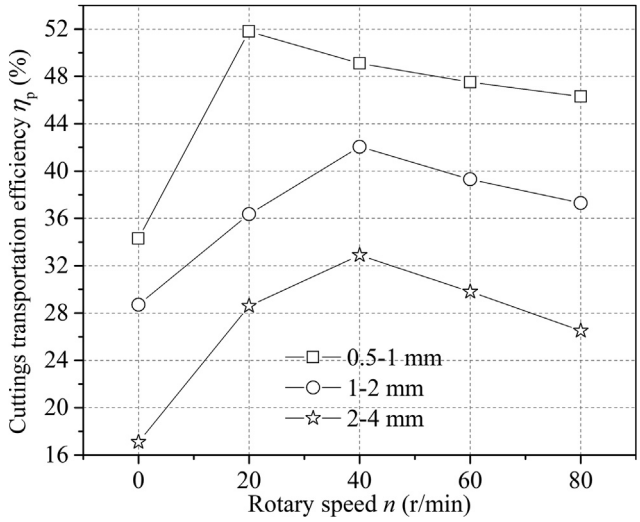

Fig. 13. Variations of η_p over rotary speed with different particle sizes.

2. Among the three theoretical correlations, Cunningham and River's (1957) correlation is most applicable to the reamer's non-cavitating performance and shows better agreement with the non-cavitating experimental data. Additionally, when the flow ratio, q, is less than 0.45, the reamer's efficiency is accurately predicted by the theoretical correlations. When q exceeds 0.45, Gosline and O'Brien (1934) as well as Lu and Zeng's (1981) correlations diverge from the experimental data and these divergences get enlarged by the flow

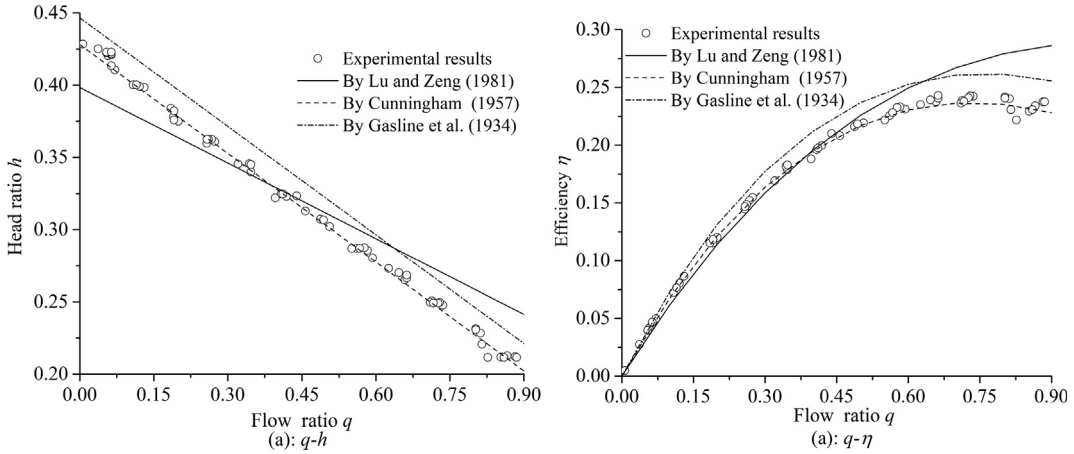

Fig. 12. Comparsions of theoretical correlations with the non-cavitating experimental data.

Table 7
Ingredients and properties of drilling fluids.

#	Ingredients	Marsh funnel viscosity (s)	Plastic viscosity (mPa·s)	Dynamic shear force (Pa)	Apparent viscosity (mPa·s)
1	Water	25	–	–	0.89
2	6%Bentonite + 0.2%Na_2CO_3 + 0.1%CMC	35.3	8	2.6	10.5
3	9%Bentonite + 0.2%Na_2CO_3 + 0.1%CMC	40.5	16	4.6	20.5

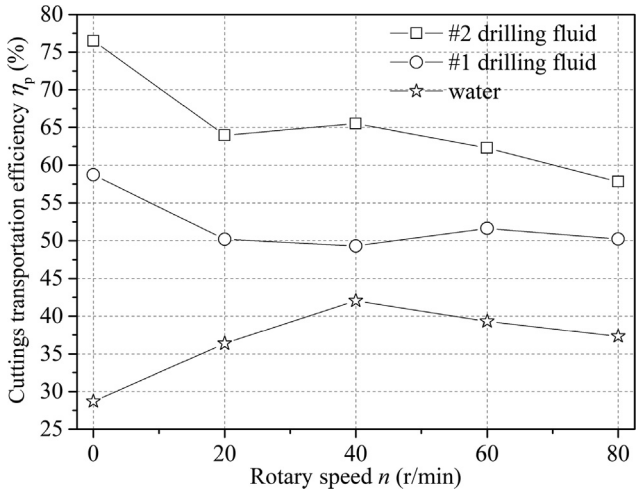

Fig. 14. Variations of η_p over rotary speed with different drilling fluids.

ratio's increase.

3. A critical rotary speed, n_c, exists at which the highest cuttings transportation efficiency is achieved. This n_c shifts from 20 r/min for 0.5–1 mm particle to 40 r/min for 2–4 mm particle. The rotary speed's increase within n_c improves the reamer's cuttings transportation ability; however, the increase beyond n_c undermines the reamer's cuttings transportation ability.
4. The reamer's cuttings transportation efficiency , η_p, is reduced by increase in particle size, and improved by using bentonite drilling fluid. Moreover, when bentonite drilling fluid is used, the highest η_p is achieved at non-rotation condition instead of at a rotary speed of 20 r/min.

Acknowledgements

This work was financially supported by the National Natural Science Foundation of China (Research on Mechanism and Application of Reverse Circulation in HDD Reaming, Project Number: 41772391)

Appendix A. Supplementary material

Supplementary data to this article can be found online at https://doi.org/10.1016/j.tust.2019.103128.

References

Ariaratnam, S.T., Harbin, B.C., Stauber, R.L., 2007. Modeling of annular fluid pressures in horizontal boring. Tunnell. Underground Space Technol. 22 (5), 610–619.
Bo, K., Yin, K., Peng, J., 2011. Reverse circulation DTH hammer drilling technique. Global Geol. 14 (4), 259–264.
Carlin, M., Ariaratnam, S.T., 2018. Comparative analysis of horizontal directional drilling pipeline practices in China vs. United States. Tunneling and Underground Space Technology, vol. 72, 174–188.
Cunningham, R.G., River, W., 1957. Jet-pump theory and performance with fluid of high viscosity. Trans. ASME. 79, 1807–1820.
Faghih, A., Yi, Y., Bayat, A., Osbak, M., 2015. Fluidic drag estimation in horizontal directional drilling based on flow equations. J. Pipeline Syst. Eng. Pract. 6 (4), 04015006.
Gan, X., Yin, K., He, J., Yin, Q., 2015. Structural design and numerical simulation on large-diameter reverse circulation drill bits with ejectors. J. Central South Univ. (Sci. Technol.) 46 (09), 3267–3273.
Gosline, J., O'Brien, M., 1934. The water jet pump. Univ. California Publ. Eng. 3, 167–190.
Kumar, P.S., Amri, B.A., Kouli, P., Gisbergen, S.V., Ferdiansyah, E., Mowat, P.M., 2005. Coiled tubing reverse circulation-an efficient method of cleaning horizontal wells in a mature pressure depleted field. SPE-92804-MS.
Li, J., Aitken, W.A., Jumawid, F., and Alingig, G., 2010. Cleaning horizontal wellbores efficiently with reverse circulation combining with wiper trip for coiled-tubing annulus fracturing application. SPE-130638-MS.
Lima Neto, I.E., Melo Porto, I., 2004. Performance of low-cost ejectors. J. Irrig. Drain. Eng. 130 (2), 122.
Liu, Q., Xia, B.R., 2009. Research on reverse circulation technology of drill dregs removal in trenchless technology. Explor. Eng. (Rock Soil Drilling Tunnell.) 2, 61–63.
Livingstone, J.I., 2007. Reverse circulation directional and horizontal drilling using concentric drill string, United States Patent No. 7, 204, 327, 2007.
Lu, H., Zeng, X., 1981. Study on liquid jet pump. Sci. China Series. A 04, 581–593.
Ma, B., Najafi, M., 2008. Development and applications of trenchless technology in China. Tunnell. Underground Space Technol. 23 (4), 476–480.
Madryas, C., Kolonko, A., Nienartowicz, B., Szot, A. (Eds.), 2017. Underground Infrastructure of Urban Areas, Wrocław 4: Proceedings of the 13th International Conference on Underground Infrastructure of Urban Areas (UIUA 2017), October 25-26. CRC Press, Poland.
Morrison, G.L., Zeineddine, T.I., Henriksen, M., Tatterson, G.B., 1987. Experimental analysis of the mechanics of reverse circulation air lift pump. Ind. Eng. Chem. Res. 26 (2), 387–391.
Munson, B.R., Young, D.F., Okiishi, T.H., 2006. Fundamentals of Fluid Mechanics, 5th ed. Wiley, Hoboken, NJ, pp. 415–422.
Rabiei, M., Yi, Y., Bayat, A., Cheng, R., 2018. Simple methods for fluidic drag estimation during pipe installation via HDD. Tunnell. Underground Space Technol. 76, 172–176.
Reddy, Y.R., Kar, S., 1968. Theory and performance of water jet pump. J. Hydraulic Div. 94, 1261–1281.
Rostami, A., Yi, Y., Bayat, A., 2017. Estimation of maximum annular pressure during HDD in noncohesive Soils. Int. J. Geomech. 17 (4), 06016029.
Rostami, A., Yi, Y., Bayat, A., Osbak, M., 2015. Predicting the plan annular pressure using the power law flow model in horizontal directional drilling. Can. J. Civ. Eng. 43 (3), 252–259.
Shu, B., Ma, B., Lan, H., 2014. Cuttings transport mechanism in a large-diameter HDD borehole. J. Pipeline Syst. Eng. Pract. 6 (4), 04014017.
Strauss, M.F., Story, S.L., Mehlhorn, N.E., 1989. Applications of dual-wall reverse-circulation drilling in ground water exploration and monitoring. Groundwater Monitor. Remediat. 9 (2), 63–71.
Turian, R.M., Hsu, F.L., Ma, T.W., 1987. Estimation of the critical velocity in pipeline flow of slurries. Powder Technol. 51 (1), 35–47.
Zhu, L.H., Huang, Y., Wang, R.H., Wang, J.Y., 2015. A mathematical model of the motion of cutting particles in reverse circulation air drilling. Appl. Math. Comput. 256, 192–202.
Zandi, I., Govatos, G., 1967. Heterogeneous flow of solids in pipelines. J. Hydraulics Div. 93 (3), 145–159.